Nonequilibrium Ribbon Model of Twisted Scroll Waves

Blas Echebarria,[1] Vincent Hakim,[2] and Hervé Henry[3]

[1]*Departament de Física Aplicada, Universitat Politècnica de Catalunya, Doctor Marañón 44, E-08028 Barcelona, Spain*
[2]*Laboratoire de Physique Statistique CNRS-UMR8550, Ecole Normale Supérieure, 24 rue Lhomond, 75231 Paris, France*
[3]*Laboratoire de Physique de la Matière Condensée CNRS-UMR7643, Ecole Polytechnique, 91128 Palaiseau, France*
(Received 26 September 2005; published 7 March 2006)

We formulate a reduced model to analyze the motion of the core of a twisted scroll wave. The model is first shown to provide a simple description of the onset and nonlinear evolution of the helical state appearing in the sproing bifurcation of scroll waves. It then serves to examine the experimentally studied case of a medium with spatially varying excitability. The model shows the role of sproing in this more complex setting and highlights the differences between the convective and absolute sproing instabilities.

DOI: 10.1103/PhysRevLett.96.098301 PACS numbers: 82.40.Ck, 82.40.Bj, 87.19.Hh, 89.75.Kd

Scroll waves, spirals tridimensional (3D) counterparts, are essential structuring elements of the dynamics of thick excitable media and are thought to play an important role in ventricular fibrillation [1,2]. This has motivated detailed examinations of their instabilities, both with chemical reactions in gels [3,4] and theoretically [5–10]. Henze *et al.* discovered that twist can destabilize a scroll straight core and lead it to adopt a helical shape [5]. This "sproing" bifurcation resembles the twist-induced instabilities of elastic rods [11,12] or of DNA [13] but has remained somewhat of a puzzle since, using long-wave expansions [6], the dynamics of a scroll core filament was found to be independent of twist [7]. Here insights gained from a numerical stability analysis [8] lead us to formulate a simple model of the core dynamics of a twisted scroll wave that is analytically tractable and agrees semiquantitatively with the results of reaction-diffusion (RD) simulations. We first show that the model provides an easy understanding as well as an accurate description of sproing. Systematic variations of electrophysiological properties are known to exist in the heart, and gradients of excitability have been shown to promote scroll wave instabilities in chemical media [3,4]. Therefore, we then choose the case of a medium with spatially varying excitability to test the usefulness of the approach beyond the simplest case of a homogeneous medium. The results show that the observed instabilities [3,4] are tightly linked to sproing and illustrate the subtleties brought by the problem nonequilibrium setting.

The center of rotation of a planar spiral becomes for a three-dimensional scroll wave the line of instantaneous center of rotations $\mathbf{R}(\sigma, t)$, where σ parametrizes this center filament and t is time. We choose to describe the scroll wave core as the ribbon $(\mathbf{R}(\sigma, t), \mathbf{p}(\sigma, t))$, where the unit vectors $\mathbf{p}(\sigma, t)$ point orthogonally from the center filament to the line of instantaneous scroll wave tips. The local rotation of the line of instantaneous tips around the center filament defines the scroll wave twist τ_w,

$$\tau_w = (\mathbf{p} \times \partial_s \mathbf{p}) \cdot \mathbf{T}, \tag{1}$$

where $\mathbf{T} = \partial \mathbf{R}/\partial s$ is the local tangent to the center filament and s its arclength (with ∂_s simply a notation for $1/|\partial \mathbf{R}/\partial \sigma|\partial_\sigma$). Starting from a straight, untwisted scroll wave, a gradient expansion [6–8,14] based on the translational and rotational invariance neutral modes shows that, at lowest order, the scroll core motion is simply driven by its center filament curvature κ [6–8]

$$\mathbf{R}_t \cdot \mathbf{N} = a_1 \kappa, \qquad \mathbf{R}_t \cdot \mathbf{B} = a_2 \kappa, \tag{2}$$

where $\mathbf{N}$ is the filament normal $\kappa \mathbf{N} = \partial \mathbf{T}/\partial s$ and $\mathbf{B} = \mathbf{T} \times \mathbf{N}$ its binormal. The case when $a_1 < 0$ is analogous to the filament having a negative line tension, and the allied instability has been extensively studied [7–10]. However, Eq. (2) leaves twist-induced instabilities unexplained, since the motion of the mean filament is not influenced by the ribbon twist [7]. Twist appears at higher orders in the gradient expansion of Refs. [6–8] but, besides being somewhat cumbersome, this rigorous approach suffers from the fundamental difficulty that sproing sets in at a finite wave number [8]. Consequently, it cannot be precisely described by a gradient expansion cut to any finite order [15]. Therefore, we find it instructive to formulate here a simple phenomenological model that captures the essence of the phenomenon and that contains only terms essential for the instability description. The filament velocity in its normal plane is written as a generalization of Eq. (2)

$$\begin{aligned}[\mathbf{R}_t]_\perp = {} & a_1 \mathbf{R}_{ss} + a_2 \mathbf{R}_s \times \mathbf{R}_{ss} + d_1 \tau_w \mathbf{R}_s \times \mathbf{R}_{sss} \\ & - d_2 \tau_w [\mathbf{R}_{sss}]_\perp - b_1 \tau_w [\mathbf{R}_{ssss}]_\perp - b_2 \mathbf{R}_s \times \mathbf{R}_{ssss},\end{aligned} \tag{3}$$

where the brackets denotes the component of the enclosed vector orthogonal to the filament tangent [e.g., $[\mathbf{R_t}]_\perp \equiv \mathbf{R_t} - (\mathbf{R_t} \cdot \mathbf{T})\mathbf{T}$]. It is worth remarking that the helical instability of an elastic ribbon with a gradient dynamics based on extension and curvature and twist energies [12] essentially depends on the a_1, b_1, and d_1 terms. The a_2, b_2, and d_2 terms describe motion in the orthogonal direction. They can appear in the present nonpotential problem due to the handedness of the spiral rotation, and their sign depends on the spiral sense of rotation. Equation (3) needs to be completed by the evolution of the ribbon twist. The twist kinematics can be adapted from previous investigations of elastic ribbons. Following Ref. [16], we note that, as one slides along the central filament at a fixed time t, the ribbon vector $\mathbf{p}$ rotates and remains orthogonal to the filament tangent $\mathbf{T}$,

$$\frac{\partial \mathbf{p}}{\partial \sigma} = \tau_w \frac{\partial s}{\partial \sigma}(\mathbf{T} \times \mathbf{p}) - \left(\frac{\partial \mathbf{T}}{\partial \sigma} \cdot \mathbf{p}\right)\mathbf{T}. \tag{4}$$

This is also true as time evolves when one stands at a fixed abscissa σ and, similarly,

$$\frac{\partial \mathbf{p}}{\partial t} = \omega(\mathbf{T} \times \mathbf{p}) - \left(\frac{\partial \mathbf{T}}{\partial t} \cdot \mathbf{p}\right)\mathbf{T}, \tag{5}$$

where ω is the local instantaneous scroll wave rotation frequency. Comparing crossed derivatives of Eqs. (4) and (5) gives as a single compatibility condition the equality of the projections of $\partial_{t,\sigma}\mathbf{p}$ and $\partial_{\sigma,t}\mathbf{p}$ on $\mathbf{T} \times \mathbf{p}$,

$$\frac{\partial}{\partial t}\left(\tau_w \frac{\partial s}{\partial \sigma}\right) = \frac{\partial \omega}{\partial \sigma} + \left(\frac{\partial \mathbf{T}}{\partial \sigma} \times \frac{\partial \mathbf{T}}{\partial t}\right) \cdot \mathbf{T}. \tag{6}$$

The kinematic equation (6) is a local description for an extensible ribbon of the well-known conversion of twist into writhe [17] associated to linking number conservation at a global level. The specific dynamics of the present problem is encoded in the twist-dependent rotation frequency ω. A good approximation for moderate twist is obtained by keeping the first twist corrections to the untwisted scroll frequency ω_0,

$$\omega = \omega_0 + c\tau_w^2 + D\partial_s \tau_w + (\mathbf{T} \cdot \partial_t \mathbf{R})\tau_w, \tag{7}$$

where the coefficients D and c can be explicitly calculated by linearization around the straight scroll wave and projection over the adjoint eigenmodes [8]. The last term in Eq. (7) is due to the apparent rotation of $\mathbf{p}$ coming from changing position along the filament. Equation (6) with (7) is equivalent to Keener's phase equation [6] and completes our formulation of the ribbon model. In the following, this simplified model is compared to simulations of RD equations in the form [18]

$$\begin{aligned} \partial_t u &= \nabla^2 u + u(1-u)[u - (v+\beta)/\alpha]/\epsilon, \\ \partial_t v &= u - v, \end{aligned} \tag{8}$$

with $\alpha = 0.8$, $\epsilon = 0.025$, and different values of β. Equations (8) are simulated with an explicit second-order scheme, with $dx = 0.15$, and $dt = 5.625 \times 10^{-3}$.

Sproing.—Taking a vertical filament along the z axis and assuming small transverse X, Y deformations, Eqs. (3), (6), and (7) become to quadratic order

$$\partial_t W = a\partial_z^2 W + id\tau_w \partial_z^3 W - b\partial_z^4 W, \tag{9}$$

$$\begin{aligned} \partial_t \tau_w = {} & \partial_s(D\partial_s \tau_w) + \partial_s(c\tau_w^2) + \partial_s \omega_0 \\ & + \mathrm{Re}\{[\partial_z(\tau_w \partial_z \bar{W}) - i(\partial_z^2 \bar{W})\partial_z]\partial_t W\}, \end{aligned} \tag{10}$$

where a complex notation has been used for the deformation field $W(z,t) = X(z,t) + iY(z,t)$, and the constants a, b, d (e.g., $a = a_1 + ia_2$), and ∂_s can be approximated by $[1 - |\partial_z W|^2/2]\partial_z$. For a uniformly twisted filament in a homogeneous medium ($\omega_0 = \mathrm{cst}$), the linear modes $W(z,t) = e^{ikz+\Omega t}$, correspond to helices of pitch k. Their dispersion relation is obtained from Eq. (9) as

$$\Omega = -ak^2 + d\tau_w k^3 - bk^4. \tag{11}$$

With appropriate constants a, b, d, it is similar to the dispersion relation obtained from RD equation (8) [Figs. 1(a) and 1(b)]. A secondary local maximum appears away from $k = 0$ when $\tau_w = 4/3\sqrt{2a_1 b_1/d_1^2}$. In a large box, instability sets in at the critical twist $\tau_w^c = 2\sqrt{a_1 b_1/d_1^2}$, with the pitch of the allied helix equal to $k_c = \sqrt{a_1/b_1}$. The mode k becomes unstable above $\tau_{w,k}^c$ when $\mathrm{Re}[\Omega(k)] > 0$. For a homogeneous twist τ_w slightly above $\tau_{w,k}^c$, the radius $R(t)$ of a helix of pitch k grows as

$$R_t = \gamma_k(\tau_w - \tau_{w,k}^c)R, \tag{12}$$

where $\gamma_k = \mathrm{Re}[\partial\Omega(k)/\partial\tau_w] = d_1 k^3$. Saturation of the instability comes from the coupling between twist and bending described by Eq. (10). For an helical mode of pitch k and time dependent but homogeneous twist and radius, the partial s derivative terms of Eq. (10) vanish. The last and only remaining term is equal to $-k^2(\tau_w + k)RR_t$, so integration of Eq. (10) shows that the twist τ_w decreases with the helix radius,

$$\tau_w = \tau_w^0 - (\tau_w^0 + k)k^2 R^2/2, \tag{13}$$

where τ_w^0 is the initial twist of the straight scroll, and we have assumed $(Rk)^2 \ll 1$ [19]. Comparison of Eqs. (12) and (13) describes sproing as a supercritical bifurcation

$$R_t = \gamma_k(\tau_w^0 - \tau_{w,k}^c)R - \frac{\gamma_k}{2}(\tau_w^0 + k)k^2 R^3. \tag{14}$$

The deformation of the center filament decreases the initial twist until the critical value $\tau_w = \tau_{w,k}^c$ is reached, at which point the driving force for the instability disappears. The final helix radius is $R = [2(\tau_w^0 - \tau_{w,k}^c)/(\tau_w^0 + k)k^2]^{1/2}$ (with $k = k_c$ in a large box).

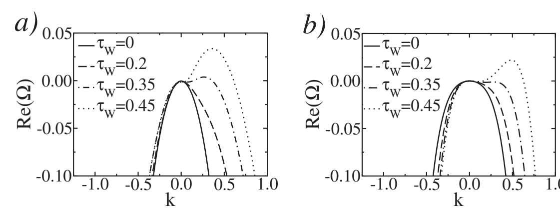

FIG. 1. (a) Dispersion relations obtained from a direct linear stability analysis of a twisted scroll wave of Eq. (8) [8], with $\alpha = 0.8$, $\epsilon = 0.025$, and $\beta = 0.01$, and (b) from Eq. (9), with $a = 0.2 + 0.2i$, $d = 3.5 + i$, and $b = 2 + i$, chosen to give a semiquantitative overall agreement between the two sets of curves. Above a critical twist, $\mathrm{Re}(\Omega)$ is positive for k around a nonzero k_c, and the straight scroll becomes unstable to a finite wave number Hopf instability. Since the instability occurs at finite wavelength, a better fit at $k = 0$ (using the exact value of a [8]) typically deteriorates the overall fit.

These analytic results compare well to results of RD simulations with periodic boundary conditions (BC) in the z direction to enforce linking number conservation [20]. As previously reported [8], sproing is found to be a supercritical bifurcation, and the twist of a bifurcated helix is very close to the critical one, in good agreement with the above findings. In large systems, as for oscillatory media [21], the helices resulting from sproing may be unstable to secondary Hopf instabilities [8], which appear sensitive to higher order nonlinearities not included in Eq. (3). These can be described by amplitude equations for the coupled helix amplitude and excess local linking number. The equations can be derived from the reduced model or directly from the RD equation (8) and take a form similar to other cases with a conservation law [22]. In simulations of Eq. (8), these secondary instabilities typically result in other helices with smaller wave number or in modulated structures.

Inhomogeneous twist.—Most experimental situations correspond to imposing free nonflux BC on Eq. (8) rather than periodic ones. These do not conserve total linking number, and an initially twisted scroll wave untwists [3] in a homogeneous medium. Spatial variations of excitability do, however, promote twist formation. Figure 2 shows RD simulations for a straight vertical filament, with nonflux BC, and either a jump [Fig. 2(a)] or a linear gradient [Fig. 2(b)] of the value of β in the z direction. For moderate variations of β, the initial untwisted core remains straight but evolves toward a final twisted and steadily rotating configuration. The different natural spiral rotation frequencies $\omega_0(z)$ create phase differences between different heights z, which, together with the rotation frequency increase with twist [Eq. (7)], lead to a steady state. The resulting distribution of twist can be computed, either analytically or numerically, from the model equation (10) using the appropriate source term $\partial_z \omega_0$. The calculated distribution of twist agrees remarkably well with the RD

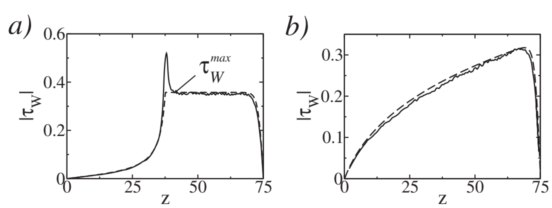

FIG. 2. Distributions of twist along a straight filament in simulations of RD equation (8) (solid line) and given by Eq. (10) (dashed line). (a) Jump of excitability obtained by taking $\beta(z) = \beta_b + (\beta_t - \beta_b)\Theta(z - L/2)$ in Eq. (8) or in the model by taking the allied spiral frequency jump $\omega_0 = \omega_b + (\omega_t - \omega_b)\Theta(z - L/2)$. (b) Linear gradient of excitability: $\beta(z) = \beta_b + (\beta_t - \beta_b)z/L$ in Eq. (8) or $\omega_0 = \omega_b + (\omega_t - \omega_b)z/L$ for the model. The parameters are the same as in Fig. 1, with $\beta_b = 0.01$, $\beta_t = 0.03$, $\omega_b = 1.80$, $\omega_t = 1.696$, and coefficients $D = 0.578$, $c = 0.720$, at the bottom, and $D = 0.614$, and $c = 0.856$, at the top, with equivalent expressions. This gives a theoretical prediction of $\tau_w^{\max} \simeq (\Delta\omega_0/c)^{1/2} = 0.35$ in (a). Here and in the following, we plot twist in absolute values.

simulations as shown in Fig. 2. For definiteness, we focus on the case of a medium with an excitability jump. In the RD equation (8), we fix $\beta_b = 0.01$ in the medium bottom half and take $\beta = \beta_t > \beta_b$ in the less excitable top half. When the jump in excitability is larger than a critical value, the straight scroll becomes unstable, very similarly to what is observed in experiments [3,4,23]. The instability is slightly subcritical and the resulting structures modulated helices (Fig. 3). To clearly relate this instability to sproing, we consider now the limit of large systems. Then, for a moderate jump of excitability, the scroll core is straight and its frequency is basically set by the domain most excitable half where the scroll twist is negligible. The scroll twist $\tau^{\max}$ in the domain less excitable half is almost constant and simply determined by the frequency jump $\Delta\omega_0$ between the two domain parts, $\tau_w^{\max} \simeq (\Delta\omega_0/c)^{1/2}$. When $\tau_w^{\max}$ reaches the sproing threshold, for a large enough jump, one could expect sproing to set in with the center filament taking the shape of a helix of constant radius in the low excitability region and radius decreasing to zero in the higher excitability part. However, the instability onset differs from the sproing threshold in a homogeneous system, even when $L \to \infty$ [Fig. 4(a)]. Furthermore, the bifurcated filament radius decreases exponentially also in the region of constant twist [Fig. 4(b)]. In order to clarify the phenomenon, we have analyzed the ribbon model in this geometry. We have solved the eigenvalue problem given by Eq. (9), with the distribution of twist calculated with Eq. (10) (with constant values of $D = 0.578$ and $c = 0.72$). Similarly to RD simulations, an instability develops in the region of constant twist when $\tau_w^{\max}$ is large enough, but its threshold differs from the sproing threshold for periodic domains [Fig. 4(c)]. The instability is nonetheless related to sproing. The reason is that periodic BC allow the growth of convective instabilities that decay with nonflux BC. For a complex growth rate Ω, four complex wave numbers $k_i(\Omega)$ satisfy the dispersion relation Eq. (11). The relevant sproing absolute spectrum, for a given constant twist in a large domain, lies on the curve of complex Ω such that $\mathrm{Im}[k_2(\Omega)] = \mathrm{Im}[k_3(\Omega)]$, with the k_i ordered by increasing the imaginary part [24,25]. For low twist, this curve lies entirely in the $\mathrm{Re}(\Omega) < 0$ half plane. The absolute instability threshold twist, for which the curve crosses the Ω imaginary axis [26], coincides with the large L limit

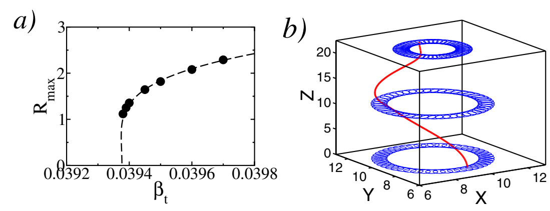

FIG. 3 (color online). (a) Center filament maximal radius vs β_t. The straight scroll becomes unstable at $\beta_t^c \simeq 0.039\,39$, resulting in a small hysteresis. (b) A 3D view of the solution for $\beta_t = 0.0399$.

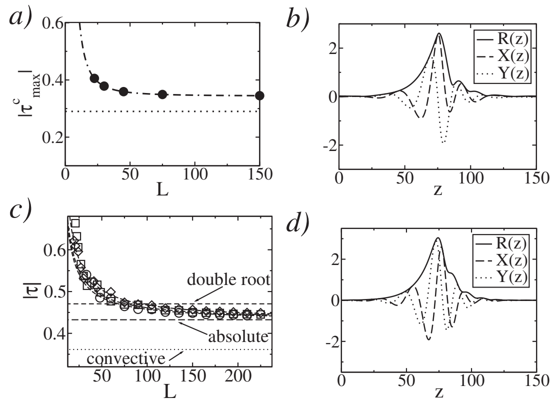

FIG. 4. (a) Instability onset vs domain size L, for domains with a jump in excitability. For fixed L, β_t is increased until the system becomes unstable. The corresponding critical twist (solid circles) is plotted together with the fit (dashed line): $\tau^c_{\max} = 0.344 + 31.3/L^2$. For comparison, the onset of sproing for periodic BC ($\tau^c_w \simeq 0.29$) is also shown (dotted line), for $\beta = 0.03$, that corresponds to the critical value of β_t in a large system. (b) Solutions for $\beta_b = 0.01$ and $\beta_t = 0.031$. (c) Model critical twist obtained by solving the eigenvalue problem vs L for the distribution of twist shown in Fig. 2(a) (diamonds), a constant twist in half of the system (squares), and vs $L/2$ for a constant twist in the whole system (circles). For comparison, we also show the onset of convective (dotted line), absolute instability (long-dashed line), and the onset obtained with the double root criterion (short-dashed line). (d) Critical modes obtained from the eigenvalue problem, using the distribution of twist, for $L = 150$.

of $\tau_c(L)$ as shown in Fig. 4(c). The most unstable modes at threshold are two counterpropagating waves, with the same spatial growth rate, and nonzero group velocity. The similarity between the critical modes for the ribbon model and the RD equation [Fig. 4(d)] further shows that sproing is also a likely explanation of the latter case and of the experimental observations [3,4].

In conclusion, the proposed ribbon model provides a semiquantitative description of the motion of twisted scroll waves and a clear understanding of several features that are difficult to extract directly from RD equations. This will hopefully help to further analyze scroll wave dynamics in complex media and to better assess the effects of gradients of electrophysiological properties and other complicating features in the cardiac muscle.

B. E. acknowledges financial support by MCyT (Spain) and by MEC (Spain), under Project No. FIS2004-02570.

[1] See, e.g., the Focus issue on fibrillation in normal ventricular myocardium [Chaos **8**, 1 (1998)].
[2] A. T. Winfree, Science **266**, 1003 (1994).
[3] A. M. Pertsov, R. R. Aliev, and V. I. Krinsky, Nature (London) **345**, 419 (1990); S. Mironov *et al.*, J. Phys. Chem. **100**, 1975 (1996).
[4] U. Storb *et al.*, Phys. Chem. Chem. Phys. **5**, 2344 (2003).
[5] C. Henze, E. Lugosi, and A. T. Winfree, Can. J. Phys. **68**, 683 (1990).
[6] J. P. Keener, Physica (Amsterdam) **31D**, 269 (1988).
[7] V. N. Biktashev, A. V. Holden, and H. Zhang, Phil. Trans. R. Soc. A **347**, 611 (1994).
[8] H. Henry and V. Hakim, Phys. Rev. Lett. **85**, 5328 (2000); Phys. Rev. E **65**, 046235 (2002).
[9] S. Alonso, F. Sagués, and A. S. Mikhailov, Science **299**, 1722 (2003).
[10] R. M. Zaritski, S. F. Mironov, and A. M. Pertsov, Phys. Rev. Lett. **92**, 168302 (2004), and references therein.
[11] A. E. H. Love, *A Treatise on the Mathematical Theory of Elasticity* (Dover, New York, 1944); A. Goriely and M. Tabor, Phys. Rev. Lett. **77**, 3537 (1996).
[12] R. E. Goldstein, T. R. Powers, and C. H. Wiggins, Phys. Rev. Lett. **80**, 5232 (1998).
[13] G. Charvin *et al.*, Contemp. Phys. **45**, 383 (2004).
[14] M. Gabbay, E. Ott, and P. N. Guzdar, Phys. Rev. Lett. **78**, 2012 (1997); Physica (Amsterdam) **118D**, 371 (1998).
[15] For a small positive filament tension $0 < a_1 \ll 1$, sproing occurs for small twist $\tau_w \sim a_1$ and small wave numbers k. Although the dispersion relation could be consistently reduced to a fourth-order polynomial in k in this limit, this is not pursued here since a resonance with the meander modes renders this parameter regime quite small, as shown in H. Henry, Phys. Rev. E **70**, 026204 (2004).
[16] I. Klapper and M. Tabor, J. Phys. A **27**, 4919 (1994).
[17] R. D. Kamien, Rev. Mod. Phys. **74**, 953 (2002).
[18] D. Barkley, Physica (Amsterdam) **49D**, 61 (1991).
[19] Equation (13) can be directly obtained from linking number conservation. The initial straight filament has zero writhe and total twist $\mathcal{T}^i_w = L\tau^0_w/(2\pi)$. The final helix has a writhe $\mathcal{W}_r = kL\{1 - [1 + (Rk)^2]^{-1/2}\}/(2\pi)$ and a total length $L[1 + (Rk)^2]^{1/2}$. So its local twist is $\tau_w = 2\pi(\mathcal{T}^i_w - \mathcal{W}_r)/\{L[1 + (Rk)^2]^{1/2}\}$. Expansion for $(Rk)^2 \ll 1$ gives back Eq. (13) and shows that both the filament length increase and the creation of writhe contribute to decrease the local twist.
[20] See EPAPS Document No. E-PRLTAO-96-007611 for additional figures. For more information on EPAPS, see http://www.aip.org/pubservs/epaps.html.
[21] G. Rousseau, H. Chaté, and R. Kapral, Phys. Rev. Lett. **80**, 5671 (1998).
[22] See, e.g., H. Riecke, in *Pattern Formation in Continuous and Coupled Systems*, edited by M. Golubitsky *et al.*, IMA Volumes in Mathematics and its Applications Vol. 115 (Springer, New York, 1999).
[23] The scroll wave core was observed to break in Refs. [3,4], presumably due to collisions with the lateral boundaries.
[24] A. G. Kulikovskii, J. Appl. Math. Mech. **30**, 180 (1966); see also L. D. Landau and E. M. Lifschitz, *Physical Kinetics* (Pergamon, Oxford, 1981), Sec. 65.
[25] B. Sandstede and A. Scheel, Physica (Amsterdam) **145D**, 233 (2000).
[26] This condition differs from the zero-group-velocity criterion [$\partial\Omega/\partial k = 0$, $\mathrm{Re}(\Omega) = 0$] [see, e.g., S. M. Tobias, M. R. E. Proctor, and E. Knobloch, Physica (Amsterdam) **113D**, 43 (1998)] that requires slow spatial variations or a Landau-Ginzburg–like dispersion relation.